A Soft Detector with Good Performance/Complexity Trade-Off for a MIMO System

Jianhua Liu

Department of Electrical and Computer Engineering, University of Florida, P.O. Box 116130, Gainesville, FL 32611-6130, USA
Email: jhliu@dsp.ufl.edu

Jian Li

Department of Electrical and Computer Engineering, University of Florida, P.O. Box 116130, Gainesville, FL 32611-6130, USA
Email: li@dsp.ufl.edu

We present a hybrid soft detector that has a good performance/complexity trade-off for a multiple-input multiple-output (MIMO) wireless communication system with known channel information. The new soft detector combines the merits of a simple unstructured least-squares (LS)-based soft detector and a list sphere decoder (LSD)-based soft detector for data bit detection. The former is computationally much more efficient than the latter at the cost of poorer performance. The poor performance of the former occurs mainly when the channel matrix is ill-conditioned. Whenever this happens, we use the LSD-based soft detector in the hybrid soft detector; otherwise, we use the LS-based one. Moreover, we provide a tight radius for a sphere decoder, a hard detector, via using the output of an LS-based hard detector. These two hard detectors are needed to determine if LS or LSD should be used in the hybrid soft detector. As an application example, we consider doubling the maximum data rate of the IEEE 802.11a conformable wireless local area networks by a MIMO system with two transmit and two receive antennas. For this application, the new soft detector is about 10 times faster than the LSD-based one and is about 10 times slower than the LS-based one. Yet the packet error rate due to using the new soft detector is quite close to that of using the LSD-based one.

Keywords and phrases: BLAST, MIMO, soft detector, convolutional codes, OFDM, WLAN.

1. INTRODUCTION

High transmission data rate is of particular importance for future wireless communication services. One promising way of increasing the transmission data rate is to deploy multiple antennas at both the transmitter and receiver ends to exploit the huge channel capacity offered by such a system in a multipath-rich environment [1, 2]. The corresponding system is referred to as a multiple-input multiple-output (MIMO) wireless system.

In practical communication systems, forward error correction codes, such as the convolutional code, are often used to lower the transmission error rate to an acceptable level [3, 4] by adding redundancy in the transmission. Soft detectors have been preferred to hard detectors since the former can lead to better detection/decoding performance. For the single-input single-out (SISO) systems, soft detectors have been well studied [3, 4]. Lately, much attention has been paid to the soft detectors for the MIMO systems.

The space-time bit-interleaved coded modulation (STBICM) scheme [5, 6] seems to be the best (in terms of performance) soft detector for a Bell-lab layered space-time

(BLAST) system [7, 8, 9], an especially attractive form of the MIMO systems. However, STBICM can only be implemented via the extremely inefficient brute-forth search. In practice, soft detectors with good performance/complexity trade-offs are desired.

Among the other existing soft detectors, the following two are particularly attractive. One is the unstructured least-squares (LS)-based soft detector of [10], which focuses more on the computational efficiency side. The other is the list sphere decoder (LSD)-based soft detector of [11], which focuses more on the performance side. The former is very simple since, for example, it decouples a multidimensional QAM symbol detection into multiple one-dimensional QAM symbol detections. However, the performance of this detector can be poor, especially when the channel matrix is ill-conditioned. The latter has a performance close to that of STBICM with a significantly improved computational efficiency; it is based on the STBICM principle but searches in a small sphere, via modifying the sphere decoder (SPD), which is a hard detector [12]. (SPD is an efficient algorithm to implement the computationally expensive maximum-likelihood (ML) hard detector.) However, the LSD-based soft

detector still requires orders of magnitude with more computations than its LS-based counterpart.

In this paper, we combine the merits of the LS- and LSD-based soft detectors to obtain a new soft detector, referred to as the hybrid soft detector, which has a better performance than the LS-based one and a higher computational efficiency than the LSD-based one. The poor performance of the LS-based soft detector is mainly due to providing poor soft information to the Viterbi decoder as a result of the channel matrix being ill-conditioned. Whenever this happens, we use the LSD-based soft detector in the new hybrid soft detector; otherwise, we use the LS-based one. To decide if LS or LSD should be used in the hybrid detector, we check to see whether or not the output of the LS-based hard detector is the same as the output of SPD. If so, we choose LS; otherwise, we use LSD. To further improve the computational efficiency, we provide a tight radius for SPD based on the output of the LS-based hard detector.

As an example, we consider doubling the maximum data rate of the IEEE 802.11a [13] conformable wireless local area networks (WLANs) by a BLAST system with two transmit and two receive antennas. At the receiver, we use soft detectors for data bit detection. We compare the performance of the new hybrid soft detector with that of the LS- and LSD-based soft detectors. The hybrid detector is about 10 times faster than the LSD-based one and is about 10 times slower than the LS-based one. Yet the packet error rate (PER) due to using the hybrid soft detector is quite close to that of using the LSD-based one.

The remainder of this paper is organized as follows. Section 2 describes the channel encoding and decoding for a BLAST system that employs the convolutional encoder. Section 3 gives the data model and formulates the soft information, that is, bit metric. Section 4 presents the proposed new hybrid soft detector. Simulation results are given in Section 5. Finally, we provide our comments and conclusions in Section 6.

2. CHANNEL CODING

Consider a BLAST system with M transmit and N ($N \geq M$) receive antennas, as shown in Figure 1. Figures 2 and 3, respectively, show the diagrams of the BLAST transmitter and receiver. At the transmitter, a convolutional encoder (CC) is employed, and an interleaver is used to break the memory of *bad channels* of the transmission. At the receiver, a deinterleaver is used before the convolutional (channel) decoder, for example, the Viterbi algorithm, to recover the order of the coded bit sequence. A $1 : M$ DEMUX and $M : 1$ MUX pair is used at the transmitter and receiver, respectively, to accommodate the BLAST scheme.

At the transmitter, as shown in Figure 2, the CC, which has a constraint length K_C, takes a block (also called packet) of bits $\mathbf{d} = \{d_1, d_2, \ldots, d_K\} \in \{-1, +1\}^{1 \times K}$ [with $(K_C - 1)$ (-1)'s at the tail to reset the CC] as its input and gives a larger block of bits $\mathbf{u} = C(\mathbf{d}) = \{u_1, u_2, \ldots, u_{\check{K}}\} \in \{-1, +1\}^{1 \times \check{K}}$ as its output, where -1 and $+1$ denote the binary digits 0
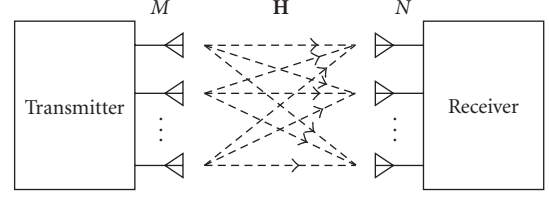

FIGURE 1: Diagram of a MIMO system.

and 1, respectively. The CC coding rate is then defined as $R_C = K/\check{K}$. We can puncture the CC output block $\mathbf{u}$ to obtain a smaller block of bits $\mathbf{v} = \{v_1, v_2, \ldots, v_{\tilde{K}}\} \in \{-1, +1\}^{1 \times \tilde{K}}$ ($\tilde{K} < \check{K}$) to increase the transmission data rate. The puncturing rate is $R_P = \tilde{K}/\check{K}$, and the coding rate of the punctured CC is $R = R_C/R_P = K/\tilde{K}$. The output $\mathbf{v}$ of the (punctured) CC is then fed to the interleaver whose output is denoted as $\check{\mathbf{v}} = \{v^{(1)}, v^{(2)}, \ldots, v^{(\tilde{K})}\} \in \{-1, +1\}^{1 \times \tilde{K}}$. Let $K' = \tilde{K}/M$ be an integer. Then the outputs of the $1 : M$ DEMUX are M independent layers, denoted as $\check{\mathbf{v}}_m = \{v_m^{(1)}, v_m^{(2)}, \ldots, v_m^{(K')}\} \in \{-1, +1\}^{1 \times K'}$, $m = 1, 2, \ldots, M$. The modulator maps each layer of the bits into data symbols through the mapping $f : \{-1, +1\}^{1 \times B} \rightarrow \mathcal{C}$, where $\mathcal{C}$ denotes the data symbol constellation and $B = \log_2 |\mathcal{C}|$ is the number of bits represented by a data symbol. Let $\bar{K} = K'/B$ be an integer, which is the number of data symbols in each layer. Then the outputs of the modulators can be denoted as $\check{\mathbf{x}}_m = \{x_m^{(1)}, x_m^{(2)}, \ldots, x_m^{(\bar{K})}\}$, $m = 1, 2, \ldots, M$. Finally, the $M \times 1$ data symbol vector $\mathbf{x}^{(\bar{k})} = [x_1^{(\bar{k})} \ x_2^{(\bar{k})} \ \cdots \ x_M^{(\bar{k})}]^T$, where $(\cdot)^T$ denotes the transpose, is transmitted through the M transmit antennas at the same time, with $\bar{k}$ denoting the time index, $\bar{k} = 1, 2, \ldots, \bar{K}$. The bits corresponding to $\mathbf{x}^{(\bar{k})}$ are denoted as a $BM \times 1$ vector $\mathbf{b}^{(\bar{k})} = [b_1^{(\bar{k})} \ b_2^{(\bar{k})} \ \cdots \ b_{BM}^{(\bar{k})}]^T$, with $b_i^{(\bar{k})} \in \{-1, +1\}$, $i = 1, 2, \ldots, BM$. Note that $\mathbf{x}^{(\bar{k})}$ is a one-to-one map of $\mathbf{b}^{(\bar{k})}$, and if needed it can be written as $\mathbf{x}^{(\bar{k})} = \mathbf{x}(\mathbf{b}^{(\bar{k})})$ to stress its dependence on $\mathbf{b}^{(\bar{k})}$.

At the receiver, as shown in Figure 3, the soft detector first generates the bit metrics $\{l_1^{(\bar{k})}, l_2^{(\bar{k})}, \ldots, l_{BM}^{(\bar{k})}\}$, with $l_i^{(\bar{k})}$ being the bit metric corresponding to $b_i^{(\bar{k})}$, $i = 1, 2, \ldots, BM$, at time $\bar{k} = 1, 2, \ldots, \bar{K}$. The soft detector then rearranges the bit metrics to obtain $\{\hat{v}_m^{([\bar{k}-1]B+1)}, \hat{v}_m^{([\bar{k}-1]B+2)}, \ldots, \hat{v}_m^{(\bar{k}B)}\}$ for the bits $\{v_m^{([\bar{k}-1]B+1)}, v_m^{([\bar{k}-1]B+2)}, \ldots, v_m^{(\bar{k}B)}\}$, which were mapped to the data symbol $x_m^{(\bar{k})}$. Let $\hat{\mathbf{v}}_m = \{\hat{v}_m^{(1)}, \hat{v}_m^{(2)}, \ldots, \hat{v}_m^{(K')}\}$, $m = 1, 2, \ldots, M$, denote the bit metric sequence corresponding to the mth transmitted layer. The M bit metric sequences are combined into one longer bit metric sequence $\hat{\mathbf{v}} = \{\hat{v}^{(1)}, \hat{v}^{(2)}, \ldots, \hat{v}^{(\tilde{K})}\}$ by the $M : 1$ MUX. Passing the above bit metric sequence $\hat{\mathbf{v}}$ through the deinterleaver, we obtain the deinterleaved bit metric sequence $\hat{\mathbf{v}} = \{\hat{v}_1, \hat{v}_2, \ldots, \hat{v}_{\tilde{K}}\}$. For the punctured CC codes, we need the bit metric for each punctured bit as well before using the Viterbi algorithm. This can be done easily by using zero as the bit metric for each punctured bit. Once we get the bit metric sequence $\hat{\mathbf{u}} = \{\hat{u}_1, \hat{u}_2, \ldots, \hat{u}_{\check{K}}\}$ corresponding to the CC output $\mathbf{u}$, we can use the Viterbi algorithm to obtain the estimate $\hat{\mathbf{d}} = \{\hat{d}_1, \hat{d}_2, \ldots, \hat{d}_K\}$ of the source bit sequence $\mathbf{d}$.
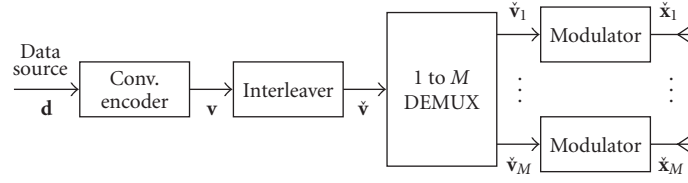
Figure 2: Diagram of a BLAST transmitter employing convolutional channel coding.
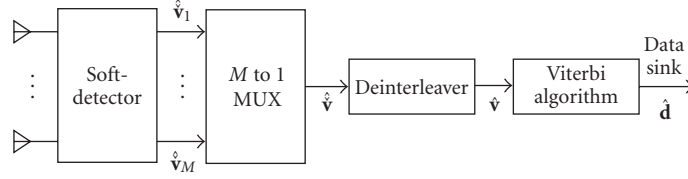

Figure 3: Diagram of a BLAST receiver employing Viterbi decoding for convolutional codes.

In the sequel, we focus on the calculation of the bit metrics for the bits in the QAM symbol, due to our WLAN application.

3. DATA MODEL AND BIT METRIC

We now give the data model and formulate the bit metric for the BLAST system.

3.1. Data model

The channel matrix of a MIMO time-varying flat Rayleigh-fading channel at time $\bar{k}$ can be written as

$$
\mathbf{H}^{(\bar{k})} = \begin{bmatrix} h_{1,1}^{(\bar{k})} & h_{1,2}^{(\bar{k})} & \cdots & h_{1,M}^{(\bar{k})} \\ h_{2,1}^{(\bar{k})} & h_{2,2}^{(\bar{k})} & \cdots & h_{2,M}^{(\bar{k})} \\ \vdots & \vdots & \ddots & \vdots \\ h_{N,1}^{(\bar{k})} & h_{N,2}^{(\bar{k})} & \cdots & h_{N,M}^{(\bar{k})} \end{bmatrix} \in \mathbb{C}^{N \times M}, \quad (1)
$$

where $h_{n,m}^{(\bar{k})}$ is the gain from the mth transmit antenna to the nth receive antenna at time $\bar{k}$, which is assumed to be known. With $\mathbf{x}^{(\bar{k})} = \begin{bmatrix} x_1^{(\bar{k})} & x_2^{(\bar{k})} & \cdots & x_M^{(\bar{k})} \end{bmatrix}^T$ denoting the $M \times 1$ QAM symbol vector being sent at time $\bar{k}$, the received signal can be written as

$$
\mathbf{y}^{(\bar{k})} = \mathbf{H}^{(\bar{k})}\mathbf{x}^{(\bar{k})} + \mathbf{n}^{(\bar{k})} \in \mathbb{C}^{N \times 1}, \quad \bar{k} = 1, 2, \ldots, \bar{K}, \quad (2)
$$

where $\mathbf{n}^{(\bar{k})} \sim \mathbf{N}(\mathbf{0}, \sigma_{\bar{k}}^2 \mathbf{I}_N)$ is the additive zero-mean white circularly symmetric complex Gaussian noise.

With an appropriate pair of interleaver and deinterleaver, the MIMO channel can be assumed to be block flat Rayleigh fading [14, 15], that is, $\mathbf{H}^{(\bar{k})}$ is constant at time $\bar{k}$ for the transmission of $\mathbf{x}^{(\bar{k})}$ but changes independently from one time index to another. In the sequel, we focus on obtaining the soft information given that we know the channel matrix $\mathbf{H}^{(\bar{k})}$, the noise variance $\sigma_{\bar{k}}^2$, and the received data vector $\mathbf{y}^{(\bar{k})}$. For notational convenience, we drop the superscript $\bar{k}$ in (2) to get

the data model

$$
\mathbf{y} = \mathbf{Hx} + \mathbf{n} \in \mathbb{C}^{N \times 1}, \quad (3)
$$

or

$$
\mathbf{y} = \mathbf{Hx}(\mathbf{b}) + \mathbf{n}. \quad (4)
$$

3.2. Bit metric

The bit metric (also known as the L-value) for the ith bit, $i = 1, 2, \ldots, BM$, is defined as

$$
l_i = \log \frac{P(b_i = +1 \mid \mathbf{y}, \mathbf{H})}{P(b_i = -1 \mid \mathbf{y}, \mathbf{H})}. \quad (5)
$$

Assuming equal probability for each data bits and using Bayes' theorem, the bit metric can be written as

$$
l_i = \log \frac{\sum_{\mathbf{b} \in \mathcal{B}_{i,+1}} P(\mathbf{y} \mid \mathbf{b}, \mathbf{H})}{\sum_{\mathbf{b} \in \mathcal{B}_{i,-1}} P(\mathbf{y} \mid \mathbf{b}, \mathbf{H})}, \quad (6)
$$

where $\mathcal{B}_{i,+1}$ and $\mathcal{B}_{i,-1}$ are the set of 2^{BM-1} bit vectors $\mathbf{b}$ with b_i being $+1$ and -1, respectively.

With the assumption of additive zero-mean white circularly symmetric complex Gaussian noise for the received data, the above equation can be written as

$$
l_i = \log \frac{\sum_{\mathbf{b} \in \mathcal{B}_{i,+1}} e^{-(1/\sigma^2)\|\mathbf{y} - \mathbf{Hx}(\mathbf{b})\|^2}}{\sum_{\mathbf{b} \in \mathcal{B}_{i,-1}} e^{-(1/\sigma^2)\|\mathbf{y} - \mathbf{Hx}(\mathbf{b})\|^2}}, \quad (7)
$$

which, by using the max-log approximation [16], can be written as

$$
\begin{aligned}
l_i &\approx \max_{\mathbf{b} \in \mathcal{B}_{i,+1}} \left\{ -\frac{1}{\sigma^2} \|\mathbf{y} - \mathbf{Hx}(\mathbf{b})\|^2 \right\} \\
&\quad - \max_{\mathbf{b} \in \mathcal{B}_{i,-1}} \left\{ -\frac{1}{\sigma^2} \|\mathbf{y} - \mathbf{Hx}(\mathbf{b})\|^2 \right\} \\
&= \frac{1}{\sigma^2} \left[\min_{\mathbf{b} \in \mathcal{B}_{i,-1}} \|\mathbf{y} - \mathbf{Hx}(\mathbf{b})\|^2 - \min_{\mathbf{b} \in \mathcal{B}_{i,+1}} \|\mathbf{y} - \mathbf{Hx}(\mathbf{b})\|^2 \right].
\end{aligned} \quad (8)
$$

This is in fact the optimal but extremely inefficient STBICM soft detector.

In the sequel, we present the hybrid soft-detector, which has a good performance/complexity trade-off, for calculating the bit metric.

4. THE PROPOSED SOFT DETECTOR

The proposed soft detector is based on the combination of the LSD- and LS-based soft detectors. As a result, before presenting the new soft detector, we summarize and comment on the merits of these two existing detectors, which are different approximations of (8) with different focuses on the performance/complexity trade-off.

4.1. The LSD-based soft detector

The LSD-based soft detector focuses mainly on the performance side of the performance/complexity trade-off. It maintains the framework of the STBICM detector and improves the efficiency of (8) by searching in much smaller subsets $\tilde{\mathcal{B}}_{i,+1} \subset \mathcal{B}_{i,+1}$ and $\tilde{\mathcal{B}}_{i,-1} \subset \mathcal{B}_{i,-1}$ with $|\tilde{\mathcal{B}}_{i,+1}| \ll 2^{BM-1}$ and $|\tilde{\mathcal{B}}_{i,-1}| \ll 2^{BM-1}$. The LSD-based soft detector is implemented in the following two steps.

Step SD1. Obtain the set $\tilde{\mathcal{B}}$ of vectors $\mathbf{b}$ which satisfies

$$\|\mathbf{y} - \mathbf{H}\mathbf{x}(\mathbf{b})\| \le d_l, \quad \forall \mathbf{b} \in \tilde{\mathcal{B}}, \tag{9}$$

by using the modified SPD algorithm that has a fixed sphere radius d_l, determined by the antenna numbers and noise variance [11].

Step SD2. For each $i = 1, 2, \dots, BM$, calculate $\tilde{\mathcal{B}}_{i,+1} = \mathcal{B}_{i,+1} \cap \tilde{\mathcal{B}}$ and $\tilde{\mathcal{B}}_{i,-1} = \mathcal{B}_{i,-1} \cap \tilde{\mathcal{B}}$ and obtain the bit metric by

$$l_i^{(\mathrm{SD})} = \frac{1}{\sigma^2} \left[\min_{\mathbf{b} \in \tilde{\mathcal{B}}_{i,-1}} \|\mathbf{y} - \mathbf{H}\mathbf{x}(\mathbf{b})\|^2 - \min_{\mathbf{b} \in \tilde{\mathcal{B}}_{i,+1}} \|\mathbf{y} - \mathbf{H}\mathbf{x}(\mathbf{b})\|^2 \right]. \tag{10}$$

At the cost of some performance degradation, the LSD-based soft detector improves the computational efficiency of the STBICM detector significantly due to limiting the search over the much smaller sets. (We do not know the exact degradation for our WLAN application since the STBICM detector is too slow to make a reasonable comparison.) However, the LSD-based soft detector is not as efficient as SPD due to the following reasons: (a) LSD in Step SD1 uses fixed sphere radius whereas SPD uses changing sphere radius that shrinks with the finding of a new point in the sphere with a shorter distance and (b) the bit metric calculation in Step SD2 needs additional computations.

4.2. The LS-based soft detector

The LS-based soft detector focuses mainly on the computational complexity side of the performance/complexity trade-off. While the LSD-based soft detector improves the efficiency of (8) by limiting the search on smaller sets, the LS-based soft detector decreases the computation of (8) by decoupling the distance $\|\mathbf{y} - \mathbf{H}\mathbf{x}\|^2$ into M separate distances,

that is, it decouples a MIMO channel into multiple SISO channels that are processed independently of each other. The LS-based soft detector has the following two main steps.

Step LS1. Ignore the discrete constellation of $\mathbf{x}$ to obtain an unstructured LS symbol estimate $\mathbf{x}^{(\mathrm{LS})}$ of $\mathbf{x}$ as

$$\begin{aligned} \mathbf{x}^{(\mathrm{LS})} &= (\mathbf{H}^H \mathbf{H})^{-1} \mathbf{H}^H \mathbf{y} \\ &= \mathbf{x} + (\mathbf{H}^H \mathbf{H})^{-1} \mathbf{H}^H \mathbf{n} \\ &\triangleq \mathbf{x} + \mathbf{e}. \end{aligned} \tag{11}$$

Step LS2. For $j = 1, 2, \dots, B$ and $m = 1, 2, \dots, M$, obtain the bit metric for each bit using the scheme (similar to (8), but for the SISO case) given in [17]

$$l_{j,m}^{(\mathrm{LS})} = \frac{1}{\sigma_m^2} \left[\min_{\mathbf{b}_m \in \mathcal{B}_{m,j,-1}} \left| x_m^{(\mathrm{LS})} - x(\mathbf{b}_m) \right|^2 - \min_{\mathbf{b}_m \in \mathcal{B}_{m,j,+1}} \left| x_m^{(\mathrm{LS})} - x(\mathbf{b}_m) \right|^2 \right], \tag{12}$$

where $\mathcal{B}_{m,j,+1}$ and $\mathcal{B}_{m,j,-1}$ are the set of 2^{B-1} bit vectors $\mathbf{b}_m \in \{-1, +1\}^{B \times 1}$ with the jth bit being $+1$ and -1, respectively, $x_m^{(\mathrm{LS})}$ is the mth element of $\mathbf{x}^{(\mathrm{LS})}$, $x(\mathbf{b}_m) \in \mathcal{C}$, and $\sigma_m^2 = \sigma^2 [(\mathbf{H}^H \mathbf{H})^{-1}]_{m,m}$ with $[\mathbf{A}]_{m,m}$ denoting the (m, m)th element of matrix $\mathbf{A}$.

We remark that for the SISO systems, we usually consider an ordinary QAM symbol as two PAM symbols (e.g., a 64-QAM symbol can be considered as two 8-PAM symbols) due to the orthogonality between the real and imaginary parts of a QAM symbol as well as the independence between the real and imaginary parts of the additive circularly symmetric Gaussian noise. The same is true for the BLAST systems employing the LS-based soft detector since the real and imaginary parts of e_m, the mth element of $\mathbf{e}$ in (12), $m = 1, 2, \dots, M$, are independent of each other, as shown below:

$$\mathrm{E}[\mathbf{e}\mathbf{e}^T] = (\mathbf{H}^H \mathbf{H})^{-1} \mathrm{E}[\mathbf{n}\mathbf{n}^T] \mathbf{H}^* \left[(\mathbf{H}^H \mathbf{H})^{-1} \right]^T = \mathbf{0}, \tag{13}$$

where we have used the fact that $\mathrm{E}[\mathbf{n}\mathbf{n}^T] = \mathbf{0}$.

The LS-based soft detector is orders of magnitude more efficient than the LSD-based soft detector due to the decoupling, as will be analyzed later. However, the performance of the former is worse than the latter (more than 2 dB for the $M = N = 2$ case for our WLAN application, to be shown by the simulation examples later).

By rounding $x_m^{(\mathrm{LS})}$, $m = 1, 2, \dots, M$, to the closest point in the constellation $\mathcal{C}$, we obtain the output of the LS-based hard detector, which will be used latter.

Note that the minimum mean-squared error (MMSE)-based soft detector is often deemed to be better than the LS-based one [18]. Although this can be true for the constant-modulus constellations, such as PSK, it is not necessarily true for QAM symbols, as suggested by our simulation results (not provided here) due to the different power levels

of the QAM symbols. Hence the LS-based soft detector is more preferable than the MMSE-based one since the former is slightly more computationally efficient than the latter.

4.3. The hybrid soft detector

The above two soft detectors provide different performance/complexity trade-offs for data bit detection, with the LSD-based one focusing on the performance and the LS-based one on the computational efficiency. In practice, it is desirable to have a soft detector that is better than the LS-based one in performance and faster than the LSD-based one in computational complexity. We show that this can be done by combining these two soft detectors, and the corresponding new detector is referred to as the hybrid soft detector.

Now, we examine what hinders the performance of the LS-based soft detector. We can readily see that when $\mathbf{H}^H\mathbf{H}$ is close to a scaled identity matrix, the bit metrics from the LS-based soft detector will not be worse than those from the LSD-based one. However, when $\mathbf{H}^H\mathbf{H}$ becomes ill-conditioned, the bit metrics from the former will be much worse than those from the latter, because of the following reasons: (a) some elements of the noise vector $\mathbf{e}$ in (11) are magnified drastically due to the poor channels and (b) useful information is lost due to the decoupling. Hence, these (bad) bit metrics corresponding to the ill-conditioned channels can be seen as the bottleneck for the performance of the LS-based soft detector. If we can identify these bad bit metrics and replace them by those from the LSD-based soft detector, we can improve the detection performance significantly.

We identify the bad bit metrics by comparing the LS-based hard detector output $\hat{\mathbf{x}}^{(\text{LS})}$ and the SPD output $\hat{\mathbf{x}}^{(\text{SPD})}$. If they are not the same, $\hat{\mathbf{x}}^{(\text{LS})}$ is more likely to have error(s) since $\hat{\mathbf{x}}^{(\text{SPD})}$ is an ML estimate, which is better than the former theoretically. In this case, the corresponding bit metrics from the LS-based soft detector are considered bad; otherwise, these bit metrics can be considered reliable.

In view of the above, we have the following steps for the hybrid soft detector.

Step HY1. Obtain the LS symbol estimate $\mathbf{x}^{(\text{LS})}$ by using (11) of Step LS1.

Step HY2. Determine the LS hard detection result $\hat{\mathbf{x}}^{(\text{LS})}$.

Step HY3. Calculate the SPD detection result $\hat{\mathbf{x}}^{(\text{SPD})}$.

Step HY4. Check the hard detection results—if $\hat{\mathbf{x}}^{(\text{LS})} = \hat{\mathbf{x}}^{(\text{SPD})}$, then go to Step HY5; otherwise, go to Step HY6.

Step HY5. Obtain bit metrics by (12) of Step LS2 based on $\mathbf{x}^{(\text{LS})}$ from Step HY1 and then stop.

Step HY6. obtain bit metrics by performing Steps SD1 and SD2 and then stop.

The computational complexity of the hybrid soft detector is dominated by SPD and the LSD-based soft detector, that is, Steps HY3 and HY6. To speed up the calculation of SPD in Step HY3, we need to consider the determination of its initial radius, which is a crucial issue for SPD. If the initial radius is too small, there will be no point ($\mathbf{x}$) in the sphere—SPD cannot find the ML solution. On the other hand, if the initial radius is too large, SPD will be very slow due to the un-

necessary additional searches. The number of the additional searches can be reduced by using a modified searching approach given in [19]. However, it complicates the algorithms itself. Here, we give a *tight* sphere radius, based on the LS-based hard-detector output $\hat{\mathbf{x}}^{(\text{LS})}$, by using

$$d_r = \|\mathbf{y} - \mathbf{H}\hat{\mathbf{x}}^{(\text{LS})}\| + \epsilon_d, \qquad (14)$$

where $\epsilon_d > 0$ is a very small value. Note that this radius will contain at least one point—the output of the LS-based hard-detector. Note also that, for most cases (98 out of 100 for the signal-to-noise-ratios (SNRs) of interest in our WLAN application, as will be shown by the simulation results in the next section), this radius contains only one point. By using this tight radius, our preliminary simulation results show that SPD can be as efficient as the interference cancellation and nulling algorithm [8] and uses only 5 times as many flops as the LS-based soft detector.

The computational complexity, in terms of flops, for each step of the LSD-based soft detector, can be estimated as follows. (We assume $M = N$ for convenience.)

Step HY1: $\mathcal{O}(M^3)$ for matrix multiplications and inversion. For example, a calculation using Matlab indicates that the number of flops is 444 for the $M = 2$ case.

Step HY2: Negligible.

Step HY3: $\mathcal{O}(M^3)$ to $\mathcal{O}(M^6)$ for SPD, depending on the SNR and B [12, 20]. For example, preliminary calculations using Matlab show that, by using the tight radius, SPD uses only 5 times as many flops as LS in Step HY1 for 64-QAM, $M = 2$, and the SNRs of interest.

Step HY4: Negligible.

Step HY5: Negligible by table checking for the PAM symbols.

Step HY6: (a) $\mathcal{O}(M^3)$ to $\mathcal{O}(M^6)$ for LSD, which, as shown by simulation results, uses typically 2 to 10 times as many flops as SPD in Step HY3, that is, 10 to 50 times as many flops as LS in Step HY1. (We use the average 25 in the sequel.) (b) $\mathcal{O}(N_C^2 BM)$ for bit metric calculation, where N_C is the number of candidates in the list for LSD and the operation of finding the minimum is performed by using the conventional bubbling algorithm; for example, for $M = 2$, $B = 6$, and $N_C = 120$ (which is typical for a good performance), this amounts to about 43200 flops (assuming $|\mathcal{B}_{i,+1}| = |\mathcal{B}_{i,-1}| = 60$, $i = 1, 2, \ldots, 12$, for convenience), which is about 95 times as many flops as LS in Step HY1.

As will be seen from the simulation results in the next section, less than 2% of the cases have different SPD and LS hard detection results. Hence, we can see that the hybrid soft detector is about

$$\underbrace{1}_{\text{LS}} + \underbrace{5}_{\text{SPD}} + 0.02 \times \left(\underbrace{25}_{\text{LSD}} + 95 \right) = 8.4 \qquad (15)$$
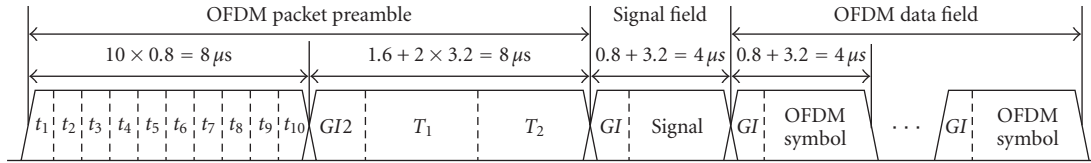
FIGURE 4: Packet structure of the IEEE 802.11a standard.

times as slow as the LS-based soft detector, which indicates that the hybrid soft detector is *about* 10 times slower than the LS-based soft detector. We can also see that the LSD-based soft detector needs 120 times as many flops as the LS-based one, which means that the hybrid soft detector is *about* 10 times faster than the LSD-based one. (This will be elaborated in the next section based on the parameters of our WLAN application.) Note that the new hybrid soft detector is more efficient for high SNRs than for low SNRs since at high SNRs the probabilities of $\hat{\mathbf{x}}^{(\mathrm{LS})} = \hat{\mathbf{x}}^{(\mathrm{SPD})}$ are high and the chances of using the computationally expensive LSD-based soft detector are low. Note also that the above analysis of the complexity is only intended to give a feeling about the efficiency of the hybrid soft detector and is by no means very accurate. More accurate analysis of the complexities, including those for SPD and LSD, is still an open topic.

We remark that the bad bit metrics can also be identified by using the condition number (CN) of $\mathbf{H}^H\mathbf{H}$, and the resulting soft detector can be referred to as the CN-hybrid soft detector. However, the CN-hybrid soft detector is inferior to its hybrid counterpart due to the following reasons. First, it is hard to determine a threshold for the CN. If the threshold is too high, many bad bit metrics from the LS-based soft detector will be used in the hybrid soft detector, which will lead to degraded performance. On the other hand, if the threshold is too low, the computationally expensive LSD-based soft detector will be used too often, which will result in increased computational complexity. Second, a large CN does not necessarily result in detection differences between SPD and the LS-based hard detectors. Neither does a small condition number guarantee the same detection result for the two hard detectors. As will be demonstrated using the simulation results in the next section, for a practical choice of CN, say 100, the CN-hybrid soft detector has a comparable $(0.06 \times (25 + 95) = 7.2$ times as many flops as LS) complexity with the hybrid soft detector; yet, the performance of the former is inferior to the latter.

5. SIMULATION RESULTS

Our results obtained under the flat fading channel condition can be readily extended to the orthogonal frequency-division multiplexing (OFDM)-based WLAN systems operating over frequency-selective fading channels [21]. This is because for each subcarrier the channel is a flat fading one. In our simulations, we follow the IEEE 802.11a 5 GHz band high-speed WLAN standard [13] whenever possible.

The OFDM-based WLAN system, as specified by the IEEE 802.11a standard, uses packet-based transmission. Figure 4 shows the packet structure specified by the standard.

Each packet consists of many OFDM symbols. Each OFDM symbol occupies 64 subcarriers, among which 48 are used for data symbols and 4 for pilot symbols. There are also 12 null subcarriers. The OFDM symbols are obtained via taking the inverse fast Fourier transform (FFT) of the data, pilots, and nulls on these subcarriers. The nominal bandwidth of the OFDM signal is 20 MHz and the I/Q sampling interval is 50 nanoseconds. Due to the fact that the modulation and demodulation are done in the frequency domain, a frequency domain bit-level interleaver is used to segment the encoded bit sequence according to the transmission data rate and to scatter them over the 48 different data-carrying subcarriers. Before interleaving, an industrial standard constraint length 7 and $R_C = 1/2$ CC is employed to code the source bit sequence. In the IEEE 802.11a standard, the maximum transmission data rate is 54 Mbps; in this case the 64-QAM constellation is used and the channel coding rate is $R = 3/4$, which comes from puncturing the $R_C = 1/2$ convolutionally encoded sequence with the puncturing rate $R_P = 2/3$. The channel is assumed to be fixed during the packet transmission.

We consider doubling the maximum 54 Mbps transmission data rate by using a BLAST system with two transmit and two receive antennas, that is, $M = N = 2$. This OFDM-based BLAST WLAN system is backward compatible with its SISO counterpart, with the packet structure shown in Figure 5. (See [21] for more detailed description of the MIMO system design.) In our simulations, each of the $MN = 4$ time domain MIMO channels is generated according to the exponential channel model [22] with the root-mean-square spreading time t_{rms} being 50 nanoseconds; the 4 channels are statistically independent of each other. After FFT at the receiver, the channel matrix for each subcarrier has the same form as in (1), with the $\bar{k}$ being the subcarrier index in this case. This subcarrier index is equivalent to the time index for time-varying flat fading channels since the channel for the OFDM-based WLANs is assumed to be fixed for the entire packet, with the changes across the subcarriers due to the delay time spreading. (Note that the intersymbol interference is avoided in the OFDM-based systems due to using the cyclic prefix [13].) We consider the case of perfect channel knowledge, where the carrier frequency offset, symbol timing, channel response, and noise variance are all known in all our simulations; in practical applications, these parameters can be estimated via applying the channel parameter estimation methods, such as those in [21, 23, 24, 25], to the packet preambles.

Due to the fact that 52 out of 64 subcarriers are used in the OFDM-based SISO WLAN system, the SNR used herein is defined as $52\sigma^2/64$ for the 64-QAM constellation whose
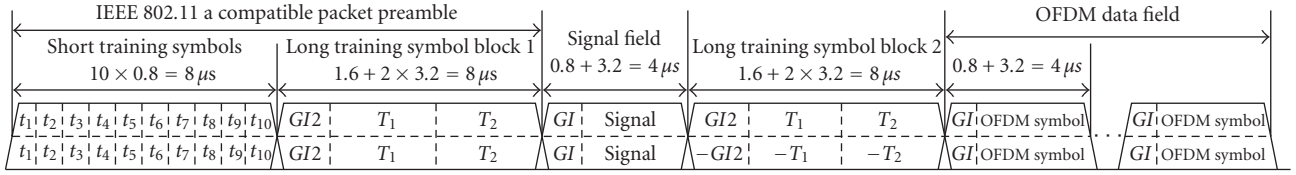

FIGURE 5: Packet structure for the OFDM-based BLAST WLAN system.
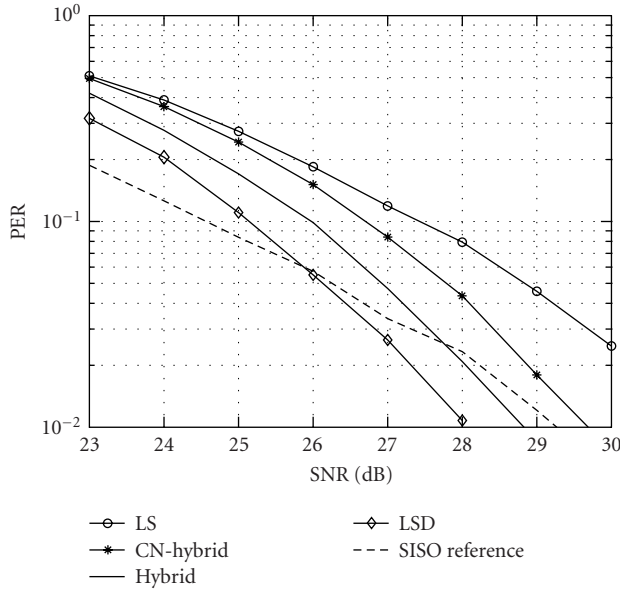
FIGURE 6: PER versus SNR comparisons for the soft detectors.

FIGURE 7: Probabilities of using LSD in the hybrid and CN-hybrid soft detectors as SNR varies.

average energy is normalized to 1. For the OFDM-based BLAST WLAN system, we keep the same total transmission power and maintain the same subcarrier structure as its SISO counterpart.

We give two simulation examples to demonstrate the performance and computational complexity of our hybrid soft detector.

Example 1 (Performance). The PER (one packet consists of 1000 bytes, which are contained in 19 OFDM symbols) is an important parameter for the OFDM-based WLAN systems. (In an OFDM-based WLAN system, even if only one error occurs, the entire packet is considered to be wrong.) In Figure 6, we show the PER comparison for the LS-based soft detector, the CN-hybrid soft detector (with CN being 100), the hybrid soft detector, and the LSD-based soft detector as a function of SNR for the OFDM-based BLAST WLAN system at the 108 Mbps data rate. We also give the PER curve of using the soft detector for the SISO system at the 54 Mbps data rate as a reference. We can see from the simulation results that for the OFDM-based BLAST WLAN system, the performance of the hybrid soft detector is close to that of the LSD-based soft detector. We can also see that the hybrid soft detector outperforms its CN-hybrid counterpart. Moreover, the PER curve of the hybrid soft detector has nearly the same slope
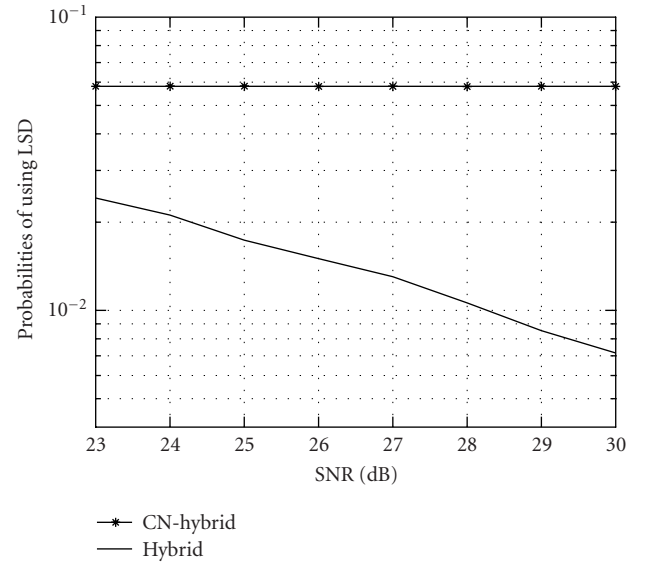
as the LSD-based one, which means that at high SNRs, the hybrid soft detector can offer much better performance than the LS-based one. Also, by comparing the solid line with the dashed line, we can see that if we use the hybrid soft detector at the receiver, we need about 1.5 dB more SNR to keep the same 10% PER (we are currently mostly interested in PERs of 10%) to double the data rate with $M = N = 2$. Note that even with the need of this 1.5 dB extra SNR, that is, 1.5 dB more total transmission power, the PER performance of the OFDM-based BLAST WLAN system with the hybrid soft detector is still impressive since even if we wish to double the transmission data rate using two separate SISO systems over two different physical channels by doubling the bandwidth, we still need 3 dB extra SNR or total transmission power. If we consider the case of 1% PER, we can double the data rate with about 0.5 dB *less* total transmission power.

Example 2 (Complexity). To facilitate the analysis of the complexity of the hybrid and CN-hybrid (with CN being 100) soft detectors, we provide a simulation example to demonstrate the probability of using the LSD-based soft detector in these soft detectors. We can see from Figure 7 that for the SNRs of interest, the probability of using the LSD-based soft detector in the CN-hybrid soft detector is about 6% and less than 2% in the hybrid soft detector.

6. CONCLUDING REMARKS

We have proposed a hybrid soft detector with a good performance/complexity trade-off by combining the LS- and LSD-based soft detectors. The combination is performed based on comparing the outputs of SPD and the LS-based hard detector. To speed up the computation of SPD, we have also provided a tight sphere radius that can be used to guarantee the finding of at least one solution. Simulation results have shown that the performance of our hybrid soft detector is close to that of the LSD-based soft detector in our WLAN application. The new detector is about 10 times faster than the LSD-based and about 10 times slower than the LS-based soft detectors.

ACKNOWLEDGMENTS

REFERENCES

[1] G. J. Foschini and M. J. Gans, "On limits of wireless communications in a fading environment when using multiple antennas," *Wireless Personal Communications*, vol. 6, no. 3, pp. 311–335, 1998.

[2] I. E. Telatar, "Capacity of multi-antenna Gaussian channels," *European Transaction Telecommunications*, vol. 10, no. 6, pp. 585–595, 1999.

[3] S. Lin and D. J. Costello, *Error Control Coding*, Prentice Hall, Englewood Cliffs, NJ, USA, 1982.

[4] J. G. Proakis, *Digital Communications*, McGraw-Hill, New York, NY, USA, 3rd edition, 1995.

[5] A. M. Tonello, "Space-time bit-interleaved coded modulation with an iterative decoding strategy," in *Proc. IEEE VTS-Fall VTC 2000. 52nd*, vol. 1, pp. 473–478, Boston, Mass, USA, 2000.

[6] J. J. Boutros, F. Boixadera, and C. Lamy, "Bit-interleaved coded modulations for multiple-input multiple-output channels," in *Proc. 6th IEEE International Symposium on Spread Spectrum Techniques and Applications*, vol. 1, pp. 123–126, Parsippany, NJ, USA, September 2000.

[7] G. J. Foschini, "Layered space-time architecture for wireless communication in a fading environment when using multiple antennas," *Bell Labs Technical Journal*, vol. 1, no. 2, pp. 41–59, 1996.

[8] G. D. Golden, G. J. Foschini, R. A. Valenzuela, and P. W. Wolniansky, "Detection algorithm and initial laboratory results using V-BLAST space-time communication architecture," *Electronics Letters*, vol. 35, no. 1, pp. 14–15, 1999.

[9] Z. Liu and G. B. Giannakis, "Layered space-time coding for high data rate transmissions," in *Proc. IEEE Military Communications Conference (MILCOM' 01)*, vol. 2, pp. 1295–1299, McLean, VA, USA, October 2001.

[10] J. Liu and J. Li, "A simple soft-detector for the BLAST system," in *Proc. Sensor Array and Multichannel Signal Processing Workshop (SAM' 02)*, pp. 159–163, Rosslyn, Va, USA, August 2002.

[11] B. M. Hochwald and S. ten Brink, "Achieving near-capacity on a multiple-antenna channel," *IEEE Trans. Communications*, vol. 51, no. 3, pp. 389–399, 2003.

[12] O. Damen, A. Chkeif, and J.-C. Belfiore, "Lattice code decoder for space-time codes," *IEEE Communications Letters*, vol. 4, no. 5, pp. 161–163, 2000.

[13] IEEE 802.11a-1999, "IEEE Standard for information technology—telecommunications and information exchange between systems—local and metropolitan area networks—specific requirements—part 11: Wireless LAN medium access control (MAC) and physical layer (PHY) specifications—amendment 1: High-speed physical layer in the 5 GHz band," IEEE, 1999.

[14] T. L. Marzetta and B. M. Hochwald, "Capacity of a mobile multiple-antenna communication link in Rayleigh flat fading," *IEEE Transactions on Information Theory*, vol. 45, no. 1, pp. 139–157, 1999.

[15] J.-C. Guey, M. P. Fitz, M. R. Bell, and W.-Y. Kuo, "Signal design for transmitter diversity wireless communication systems over Rayleigh fading channels," *IEEE Trans. Communications*, vol. 47, no. 4, pp. 527–537, 1999.

[16] J. Hagenauer, E. Offer, and L. Papke, "Iterative decoding of binary block and convolutional codes," *IEEE Transactions on Information Theory*, vol. 42, no. 2, pp. 429–445, 1996.

[17] G. Caire, G. Taricco, and E. Biglieri, "Bit-interleaved coded modulation," *IEEE Transactions on Information Theory*, vol. 44, no. 3, pp. 927–946, 1998.

[18] C. Z. W. H. Swetman, J. S. Thompson, B. Mulgrew, and P. M. Grant, "A comparison of the MMSE detector and its BLAST versions for MIMO channels," in *IEE Seminar on MIMO: Communications Systems from Concept to Implementations*, pp. 19/1–19/6, London, UK, December 2001.

[19] A. M. Chan and I. Lee, "A new reduced-complexity sphere decoder for multiple antenna systems," in *Proc. IEEE International Conference on Communications (ICC' 02)*, vol. 1, pp. 460–464, New York, NY, USA, 2002.

[20] M. O. Damen, K. Abed-Meraim, and M. S. Lemdani, "Further results on the sphere decoder," in *Proc. 2001 IEEE International Symposium on Information Theory*, pp. 1–333, Washington, DC, USA, June 2001.

[21] J. Liu and J. Li, "A MIMO system with backward compatibility for OFDM-based WLANs," *EURASIP Journal on Applied Signal Processing*, vol. 2004, no. 5, pp. 696–706, 2004.

[22] N. Chayat, "Tentative criteria for comparison of modulation methods," *Doc. IEEE 802.11-97/96*, September 1997.

[23] E. G. Larsson, G. Liu, J. Li, and G. B. Giannakis, "Joint symbol timing and channel estimation for OFDM based WLANs," *IEEE Communications Letters*, vol. 5, no. 8, pp. 325–327, 2001.

[24] J. Li, G. Liu, and G. B. Giannakis, "Carrier frequency offset estimation for OFDM-based WLANs," *IEEE Signal Processing Letters*, vol. 8, no. 3, pp. 80–82, 2001.

[25] J. Liu and J. Li, "Channel parameter estimation and error reduction for OFDM-based WLANs," to appear in *IEEE Transactions on Mobile Computing*.

Jianhua Liu received the B.S. degree in electrical engineering from Dalian Maritime University, Dalian, China, in 1984, the M.S. degree in electrical engineering from the University of Electronic Science and Technology of China, Chengdu, China, in 1987, and the Ph.D. degree in electronic engineering from Tsinghua University, Beijing, China, in 1998. From March 1987 to February 1999, he worked at the Communication, Telemetry and Telecontrol Research Institute, Shijiazhuang, China, where he was an Assistant Engineer, Engineer, Senior Engineer, and Fellow Engineer. From March 1995 to August 1998,

he was also a Research Assistant at Tsinghua University. From February 1999 to June 2000, he worked at Nanyang Technological University, Singapore, as a Research Fellow. Since June 2000, he has been a Research Assistant in the Department of Electrical and Computer Engineering at the University of Florida, Gainesville, working towards a Ph.D. degree majoring in electrical engineering and minoring in statistics. His research interests include wireless communications, statistical signal processing, and sensor array processing.

Jian Li received the M.S. and Ph.D. degrees in electrical engineering from The Ohio State University, Columbus, in 1987 and 1991, respectively. From April 1991 to June 1991, she was an Adjunct Assistant Professor with the Department of Electrical Engineering, The Ohio State University, Columbus. From July 1991 to June 1993, she was an Assistant Professor with the Department of Electrical Engineering, University of Kentucky, Lexington. Since August 1993, she has been with the Department of Electrical and Computer Engineering, University of Florida, Gainesville, where she is currently a Professor. Her current research interests include spectral estimation, array signal processing, and their applications. Dr. Li is a Member of Sigma Xi and Phi Kappa Phi. She received the 1994 National Science Foundation Young Investigator Award and the 1996 Office of Naval Research Young Investigator Award. She was an Executive Committee Member of the 2002 International Conference on Acoustics, Speech, and Signal Processing, Orlando, Florida, May 2002. She has been an Associate Editor of the IEEE Transactions on Signal Processing since 1999 and an Associate Editor of the IEEE Signal Processing Magazine since 2003. She is presently a Member of the Signal Processing Theory and Methods (SPTM) Technical Committee of the IEEE Signal Processing Society.